An Improved APFM for Autonomous Navigation and Obstacle Avoidance of USVs

Xiaohui Zhu[1,2,3][a], Yong Yue[1], Hao Ding[3,4], Shunda Wu[3], MingSheng Li[3] and Yawei Hu[3]

[1] *Department of Computer Science and Software Engineering, Xi'an Jiaotong-Liverpool University, Suzhou, Jiangsu Province, 215123, P. R. China*

[2] *Department of Computer Science, University of Liverpool, Liverpool, L69 3BX, U.K.*

[3] *School of Information Science and Technology, Nantong University, Nantong, Jiangsu Province, 226019, P. R. China*

[4] *Nantong Research Institute for Advanced Communication Technologies, Nantong, Jiangsu Province, 226019, P. R. China*

Keywords: Autonomous Navigation, Obstacle Avoidance, Improved APFM, USVs, Water Quality Monitoring.

Abstract: Unmanned surface vehicles (USVs) are getting more and more attention in recent years. Autonomous navigation and obstacle avoidance is one of the most important functions for USVs. In this paper, we proposed an improved angle potential field method (APFM) for USVs. A reversed obstacle avoidance algorithm was proposed to control the steering of USVs in tight spaces. In addition, a multi-position navigation route planning was also achieved. Simulation results in MATLAB show that the improved APFM can guide the USV to autonomously navigate and avoid obstacles around the USV during navigation. We applied the algorithm to a real USV, which is designed for water quality monitoring and tested in a real river system. Experimental results show that the improved APFM can successfully guide the USV to navigate based on the predefined navigation route while detecting both static and dynamic obstacles and avoiding collisions.

1 INTRODUCTION

With the development of sensor technology, mobile network, autonomous navigation and artificial intelligence (AI), unmanned surface vehicles (USVs) are getting more and more attention in scientific research (Liu et al., 2017), environmental missions (Polvara et al., 2018a) , military operations and civilian applications (Liu et al., 2016). Many countries, especially those with vast water resources are vigorously developing USVs (Zhou et al., 2015). US Naval Undersea Warfare Center developed the Spartan Scout USV, an advanced concept technology demonstration in 2002 (Maguer et al., 2005). In Japan, Yamaha developed two USVs, the Unmanned Marine Vehicle High-Speed UMV-H and the Unmanned Marine Vehicle Ocean type UMV-O for monitoring bio-geo-chemical parameters of oceans and atmosphere (Enderle et al., 2004). The Portuguese Dynamical Systems and Ocean Robotics Laboratory developed several marine robotic vessels(Bertram, 2008). According to practical applications and requirements, USVs have various appearances such as rigid inflatable hulls, kayaks, catamarans and trimarans (Naeem et al., 2008; Peng et al., 2009). Due to catamaran's stability in heavy-weather situations and its ample space for setting additional water quality monitoring devices, it is widely used in environmental monitoring.

Generally, USVs usually consist of three main modules: data acquisition, path planning and navigation control. Many researchers have proposed various algorithms for autonomous navigation and collision avoidance (Li et al., 2017; Wang et al., 2011; Zhang et al., 2014a). Artificial potential field method was a real-time obstacle avoidance approach (Khatib, 1986a). It use attractive force to allow robots to reach the destination and use repulsion force to keep robots away from obstacles. The resultant of these two forces can guide the robot to avoid obstacles during the navigation. The approach is widely used due to its advantages of simplicity and small computing requirement. However, it also has a disadvantage of having local optimal solutions. Borenstein proposed a vector field histogram(VFH) algorithm to achieve obstacle avoidance for fast mobile robots in cluttered environments (Borenstein and Koren, 1990). It uses a two-dimensional Cartesian histogram grid as a world

[a] https://orcid.org/0000-0003-1024-5442

Zhu, X., Yue, Y., Ding, H., Wu, S., Li, M. and Hu, Y.
An Improved APFM for Autonomous Navigation and Obstacle Avoidance of USVs.
DOI: 10.5220/0007922904010408
In *Proceedings of the 16th International Conference on Informatics in Control, Automation and Robotics (ICINCO 2019)*, pages 401-408
ISBN: 978-989-758-380-3

model. The VFH algorithm is efficient and robust. However, the size of grid cells is highly related to the computing performance. The smaller the grid cell, the clearer the environmental information is drawn, but the amount of computational time and storage space will increase exponentially. With the development of artificial intelligence (AI), AI algorithms such as neural network and particle swarm optimization were also used for autonomous navigation (Polvara et al., 2018b; Zhang et al., 2014b). However, AI algorithms usually need much more computational resources. Due to the constrained electric energy and computing resources on small USVs, it is not always available for small USVs. The angle potential field method (APFM) can guide mobile robots to reach the destination by a combined force from obstacles and the destination (Li and He, 2006).

In this paper, we review the fundamental concept of APFM in Section II. Section III introduces the improved APFM according to the particular requirement of USVs. We simulate the improved APFM in MATLAB to analysis the correctness and performance of our algorithm in Section IV. We apply the algorithm to a real USV and test in a lake in Section V. Finally, we make a conclusion in Section VI.

2 ANGLE POTENTIAL FIELD METHOD

The angle potential field method (APFM) was proposed for outdoor mobile robots in 2006 (Li and He, 2006). The APFM is based on an artificial potential field concept (Khatib, 1986b). The main idea of APFM is: each obstacle around the robot produces a resistance to the robot, and the target point produces an attraction to the robot. The accessibility of each angle for the robot is determined by the ratio of attraction and resistance. The angle with maximal accessibility is the heading for the robot.

2.1 Resistance of Obstacles

The resistance to a robot is produced by surrounding obstacles. When the linear distance D_l between an obstacle and the robot is decreased, the resistance is increased. Otherwise, the resistance is decreased. We assume D_{ms} is the minimal safety lateral distance between the robot and an obstacle for the robot to safely pass through the obstacle. The D_{ms} is defined as follows.

$$D_{ms} = \frac{1}{2} K_{ms} W \tag{1}$$

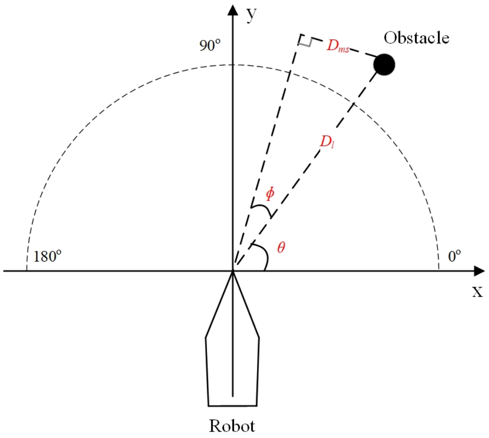

Figure 1: Risk collision area of an obstacle in the robot fixed coordinate frame.

where W is the width of the robot, K_{ms} is a coefficient to extend the safety lateral distance between the robot and an obstacle, and $K_{ms} \geq 1$.

We let θ be the angle of an obstacle in the robot fixed coordinate frame. Figure 1 shows the risk collision area of an obstacle to the robot in navigation. The risk angle ϕ for the robot is defined by the following equation.

$$\phi = argsin(\frac{D_{ms}}{D_l}) \tag{2}$$

Equation 2 means that if the heading of the robot is within the angle ϕ, the robot will collide with the obstacle. As we know that the robot may pass through the obstacle from the right or left side, the collision angle φ for the robot is shown as follows.

$$\theta - \phi \leq \varphi \leq \theta + \phi \tag{3}$$

Let D_{min} be the minimum safety linear distance between an obstacle and the robot, D_{max} be the maximum distance of obstacle detection, $K_r(\theta, \varphi)$ be the resistance of an obstacle at angle θ to the robot at angle φ. We let $K_r(\theta, \varphi)$ be a small constant when the distance D_l is larger than D_{max}. if D_l is smaller than D_{min}, it means that the robot will collide with the obstacle and we let $K_r(\theta, \varphi)$ be a infinite value. Otherwise, $K_r(\theta, \varphi)$ is inversely proportional to the difference between D_l and D_{min}. Equation 4 means that when the heading of the robot is not within the collision angle, we do not need to calculate the resistance of the obstacle. Otherwise, we should calculate the resistance $K_r(\theta, \varphi)$ and there are three situations we should consider based on the distance D_l between the robot and the obstacle.

$$K_r(\theta,\varphi) = \begin{cases} 0, \quad if \quad \varphi > \theta + \phi \quad or \quad \varphi < \theta - \phi \\ +\infty, \quad if \quad D_l < D_{min} \quad and \quad \theta - \phi \leq \varphi \leq \theta + \phi \\ \frac{1}{D_l - D_{min}}, \quad if \quad D_{min} \leq D_l \leq D_{max} \quad and \quad \theta - \phi \leq \varphi \leq \theta + \phi \\ \frac{1}{D_{max} - D_{min}}, \quad if \quad D_l > D_{max} \quad and \quad \theta - \phi \leq \varphi \leq \theta + \phi \end{cases} \tag{4}$$

We let $K_r(\varphi)$ be the maximal resistance that all obstacles in front of the robot at angle φ, which is shown in Equation 5.

$$K_r(\varphi) = \max_{\varphi \in [0\ \pi]} (K_r(\theta,\varphi)) \tag{5}$$

2.2 Abstraction of Target Point

To guide the robot to move towards the target point, we define an attraction $K_a(\varphi)$ for the target point at angle φ as follows.

$$K_a(\varphi) = \cos(\varphi - \theta_{destinaton}) \tag{6}$$

where $\theta_{destinaton}$ is the angle of the target point and φ is the heading of the robot. From Equation 6 we know that when the deviation between the heading of the robot and the destination is increased, the attraction $K_a(\varphi)$ is decreased. otherwise, $K_a(\varphi)$ will be increased.

2.3 Pass Function

Based on the maximum resistance of obstacles around the robot and the attraction of the destination to the robot, we define a pass function $K_p(\varphi)$ as follows.

$$K_p(\varphi) = \max_{\varphi \in [0\ \pi]} \left(\frac{K_a(\varphi)}{K_r(\varphi)}\right) \tag{7}$$

We know from Equation 7 that the APFM tries to find a angle φ in $[0\ \pi]$ which has maximal value of $K_p(\varphi)$. Then we should let the robot turn to that angle and move forward. The process continues until the robot reaches the target point.

3 IMPROVEMENT OF APFM

3.1 Issues in APFM

As we know that mobile robots are quite different from USVs as follows. They should be carefully considered and solved before we can apply the APFM to USVs.

- Mobile robots can accurately control or rapidly change their moving speed on land. However, affected by the wind and water flows, it is difficult for USVs to strictly and immediately control and change sailing speed.
- The steering operation of mobile robots is easy to achieve. Constrained by steering angle of the rudder and the servo, the steering operation of USVs needs much more time than mobile robots.
- When the distance between obstacles and the robot is too small for the robot to turn, the original APFM simply stops the robot. It is not acceptable when we apply this algorithm to a real USV.
- The original APFM only considers the straight path planning of a single position. To a real USV, multi-position path planning has to be achieved.
- Further research shows that there is a potential issue when there is no obstacle around the robot, which means the resistance $K_r(\varphi)$ is 0. Equation 7 indicates that when $K_r(\varphi)$ is 0, we get a maximal $K_p(\varphi)$ no matter what the value of $K_a(\varphi)$ is. It is unreasonable when there is more than one angle which has a resistance of 0. Because in this situation, we still should select an angle which has the largest attraction to the destination and drive the USV toward this angle.

3.2 Improved APFM

According to the issues proposed above, we improve the APFM as follows.

- Firstly, to simplify the speed and heading control of the USV, we assume the USV has a stable speed during navigation. It is easy to achieve in a real application by controlling the ESC to provide stable power to the motor in the USV.
- Secondly, we use a Proportional-Integral-Derivative (PID) controller to control the heading of USV. The PID controller can continuously adjust the heading of USV until it reaches the desired heading.
- Thirdly, we propose a reversed obstacle avoidance algorithm. When the distance between obstacles and the USV is too small to turn the heading of the USV, we let a position which is symmetric with the actual target point of the USV regarding the current position of the USV be the virtual target point and let the stern direction of the USV

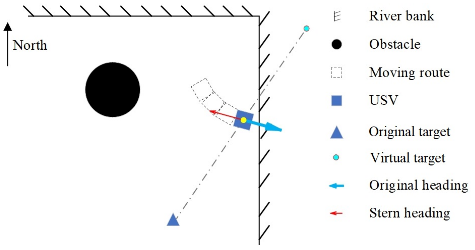

Figure 2: Reversed obstacle avoidance.

as a virtual heading. We apply the APFM again based on the virtual target point and the heading to guide the USV to move far away from obstacles. Finally, We continue the navigation process again to let the USV reach the real target point. Figure 2 shows the procedure of the reversed obstacle avoidance algorithm.

From figure 2 we know that the USV is at the corner of a river. Due to the closeness to the right bank and its current heading, the USV cannot find a way to the original target point. In this situation, the reserved obstacle avoidance algorithm will try to drive the USV back and head to the virtual target point, which is symmetric with the actual target point regarding the current position of the USV. Finally, the heading of USV is turned to the direction of the original target point, and the navigation can be continued.

- Fourthly, we extend the single position path planning to multi-position path planning. Integrated with the reversed obstacle avoidance algorithm, At first, we let the first position as the current target point for the USV. When the USV reaches the first target, we let the subsequent positions as the current target of the USV one by one. Finally, the USV can reach the final destination.

- Finally, to solve this potential issue when there is no obstacle around the USV, we set the $K_r(\varphi)$ to a very small constant when there is no resistance at angle φ. we revise Equation 4 as follows. where $0 < \omega < 1$. It is easy to know that $\omega * \frac{1}{D_{max}-D_{min}}$ is the smallest value in Equation 8, which means there is no obstacle at the angle φ for the USV. So the final heading of the USV will be determined by the attraction $K_a(\varphi)$ in Equations 6 and 7.

4 SIMULATIONS AND ANALYSIS

We assume the length and width of USV are both one meter and the turning radius of the USV is 2.5 meters. We define a 50*50 m square as a river area for the test. In addition, we let the minimum safety linear distance (D_{min}) between an obstacle and the USV be 2 meters, the maximum distance (D_{max}) for obstacle detection be 8 meters and the minimal safety lateral distance (D_{ms}) between the USV and an obstacle be 1 meter. We implemented the improved APFM in MATLAB and considered several scenarios as follows.

4.1 Obstacle Detection and Avoidance with Multiple Positions

The multi-position path planning is shown in Figure 3. We set a scenario with four navigation positions. We let the first position be the departure, and the last position be the destination respectively. Figure 4 shows the navigation process. Because obstacles are far away from the navigation route between the departure position to the first target position, the cruise track between these two positions is a straight line. Attracted by the second target position, the USV turns right and moves towards the second target position. Influenced by the resistance of the right bottom obstacle, the USV slightly turns right again to avoid the obstacle on its left side and reaches the second target position. With the attraction of the destination position at the right top, the USV turns right again and moves ahead to the destination. Affected by the resistance of the central obstacle, the USV starts to turn left when it moves close to the central obstacle. However, attracted by the destination, the USV turns slightly right but still have enough safety distance from the obstacle. Finally, it reaches the destination.

4.2 Reversed Obstacle Avoidance between Two Positions

In this simulation, we set the departure position at the right top, which is very close to the right bank of the river and the destination position at the left bottom. Similar to the previous simulation, there is an obstacle between the departure and destination positions. Figure 5 shows the simulation result.

The purple ellipse is the area where the reversed obstacle avoidance algorithm works. Figure 6 shows the detailed process of reversed obstacle avoidance. The cruise track of the USV is the blue rectangles. The grey rectangles represent the brake track of the USV when it is close to the right border. The red rectangles are the cruise track when the reversed obstacle avoidance algorithm works.

Constrained by the minimum turning radius of the USV, during the turning process, the USV is too close to the right border and cannot turn. The USV is stopped when the distance between the USV and the right border is smaller than the minimum safety

$$K_r(\theta,\varphi)=\begin{cases}\omega*\frac{1}{D_{max}-D_{min}}, & if \quad \varphi>\theta+\phi \quad or \quad \varphi<\theta-\phi\\ +\infty, \quad if \quad D_l<D_{min} \quad and \quad \theta-\phi\leq\varphi\leq\theta+\phi\\ \frac{1}{D_l-D_{min}}, \quad if \quad D_{min}\leq D_l\leq D_{max} \quad and \quad \theta-\phi\leq\varphi\leq\theta+\phi\\ \frac{1}{D_{max}-D_{min}}, \quad if \quad D_l>D_{max} \quad and \quad \theta-\phi\leq\varphi\leq\theta+\phi\end{cases} \tag{8}$$

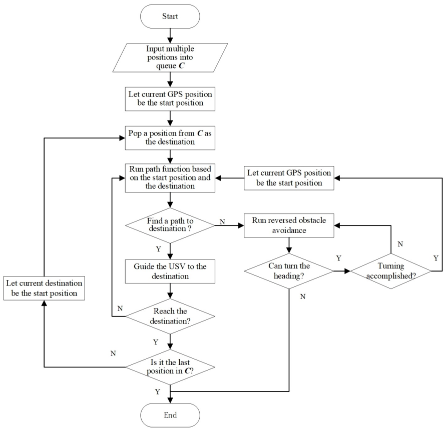
Start
Input multiple positions into queue C
Let current GPS position be the start position
Pop a position from C as the destination
Run path function based on the start position and the destination
Let current GPS position be the start position
Find a path to destination ?
N
Run reversed obstacle avoidance
Y
Guide the USV to the destination
Can turn the heading?
Y
Turning accomplished?
N
Y
N
Let current destination be the start position
N
Reach the destination?
Y
N
Is it the last position in C?
Y
End

Figure 3: Multi-position path planning.

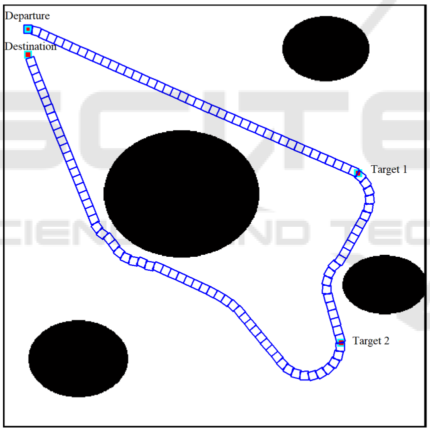

Figure 4: Obstacle detection and avoidance with multiple positions.

distance D_{min}. Then, the reversed obstacle avoidance algorithm guides the USV to go backwards and turn right. As a result, the USV leaves far away from the right border of the river and turns the heading to the destination position. Finally, the USV has enough turning radius and is guided by the improved APFM to avoid obstacles and reaches the destination position at the left bottom.

4.3 Obstacle Detection and Avoidance with Moving Obstacles

We simulate a scenario with moving obstacles. We add a referential USV with a speed of $1m/s$ as a moving obstacle and assume it can only detect static obstacles. The referential USV moves from the left position towards the right bottom position. We use red rectangles to identify the cruise track of the referential USV. Figure 7 demonstrates the process of moving obstacle detection and avoidance when two USVs meet each other. We find that when two USVs are approaching, the referential USV cannot detect the approaching of another USV and does not change its navigation route. However, the first USV can detect the referential USV, and the resistance from the referential USV to the first USV will be calculated. Affected by another resistance from the obstacle and the attraction from the immediate target position, the USV slightly turns left to avoid the collision with the referential USV and continues to go towards the destination.

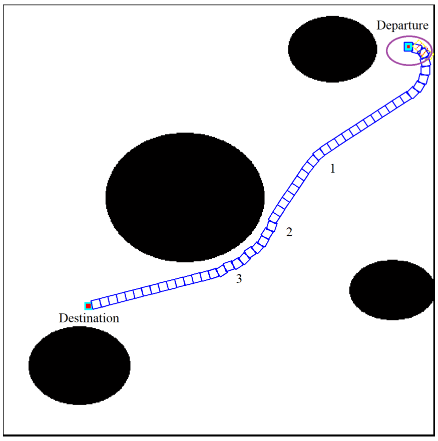

Figure 5: Reversed obstacle avoidance between two positions.

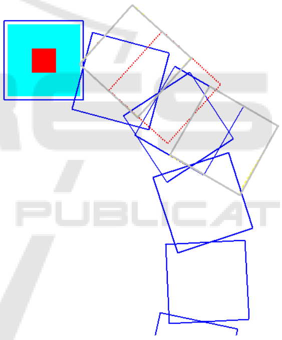

Figure 6: Enlarged image for the process of reversed obstacle avoidance.

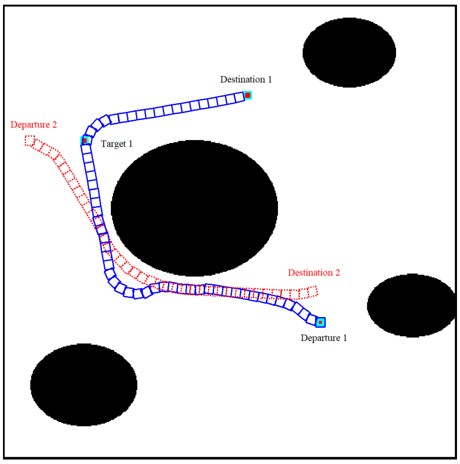

Figure 7: Obstacle detection and avoidance with moving obstacles.

5 USVS AND EXPERIMENTAL RESULTS

5.1 Architecture of USVs

We developed a USV for water quality monitoring. The main architecture of the USV is shown in Figure 8. During navigation, the USV uses a simple commercial GPS receiver to continuously obtain its positions from GPS satellites. The positioning accuracy of the GPS receiver is 1.5 meters. An inertial measurement unit (IMU) is used to obtain the USV's heading and acceleration in real time. In addition, the USV can detect surrounding obstacles protruding from the water surface using a single-line LIDAR. The detection distance of the LIDAR is 10 meters. All these data will be input to the algorithm of autonomous navigation and obstacle avoidance to guide the navigation of the USV based on a predefined navigation route. Water quality sensors deployed under the USV body collect water quality data at a regular interval. A 4G-based data transfer unit (DTU) transfers water quality data to the remote data center via the 4G mobile network and the Internet. Finally, all the water quality data are processed and saved in a database. Front end users can use a web browser or an Android APP to query and analyse water quality data respectively.

The USV is based on a catamaran. The stability, payload capacity and ease of deck access make catamarans a compelling for USVs (Manley, 2008). Figure 9 shows the main components of the USV. All the electronic devices such as the Raspberry Pi, battery, DTU and GPS are all installed in the cabin. The water quality monitoring sensors and a Doppler sensor are deployed under the USV. Both live camera and LIDAR are installed in the front of the USV.

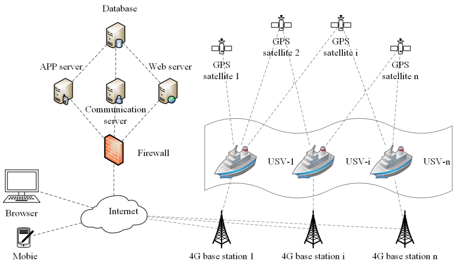

Figure 8: Architecture of USVs.

5.2 Autonomous Navigation and Obstacle Avoidance

5.2.1 Autonomous Navigation

The USV is tested in a small lake which is about 213 meters long and 196 meters wide. We select seven positions using Google map to define a polygon and zigzag navigation route respectively shown in Figures 10(a) and 10(b). The actual autonomous navigation trajectory is shown in Figures 10(c) and 10(d). Compared the actual navigation trajectory to the predefined navigation route we find that the improved APFM can guide the navigation of the USV based on the predefined navigation route. However, affected by the wind and the accuracy of the GPS receiver, there is a little deviation between the actual trajectory and the predefined route.

5.2.2 Obstacle Avoidance

We set another polygon route with five positions to test the function of obstacle avoidance. We use two balloons as static obstacles and one remote controlled ship (RC ship) as a dynamic obstacle during the navigation. The navigation route and the experimental scenario are shown in Figure 11.

We use a RC ship to simulate a dynamic obstacle. When the USV is navigating from the third position to the fourth position, we remotely control the RC ship move towards the USV to verify whether the USV can detect the dynamic obstacle and avoid the collision or not. From Figure 11(c) we find that controlled by the algorithm of autonomous navigation and obstacle avoidance, the USV can autonomously navigate based on the predefined navigation route.

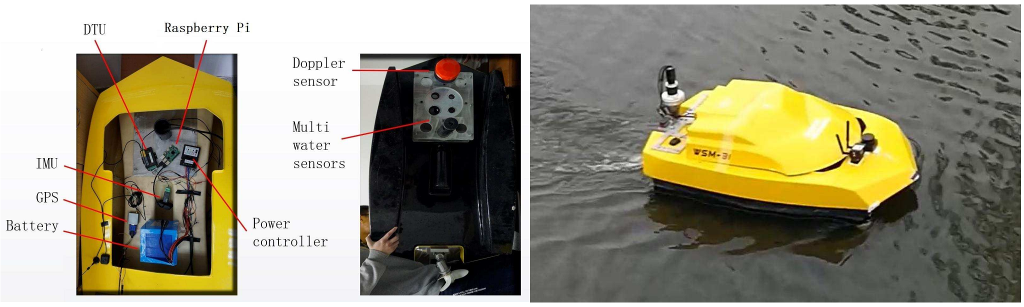

(a) Components of the USV

(b) Overall appearance of the USV

Figure 9: Main components of the USV.

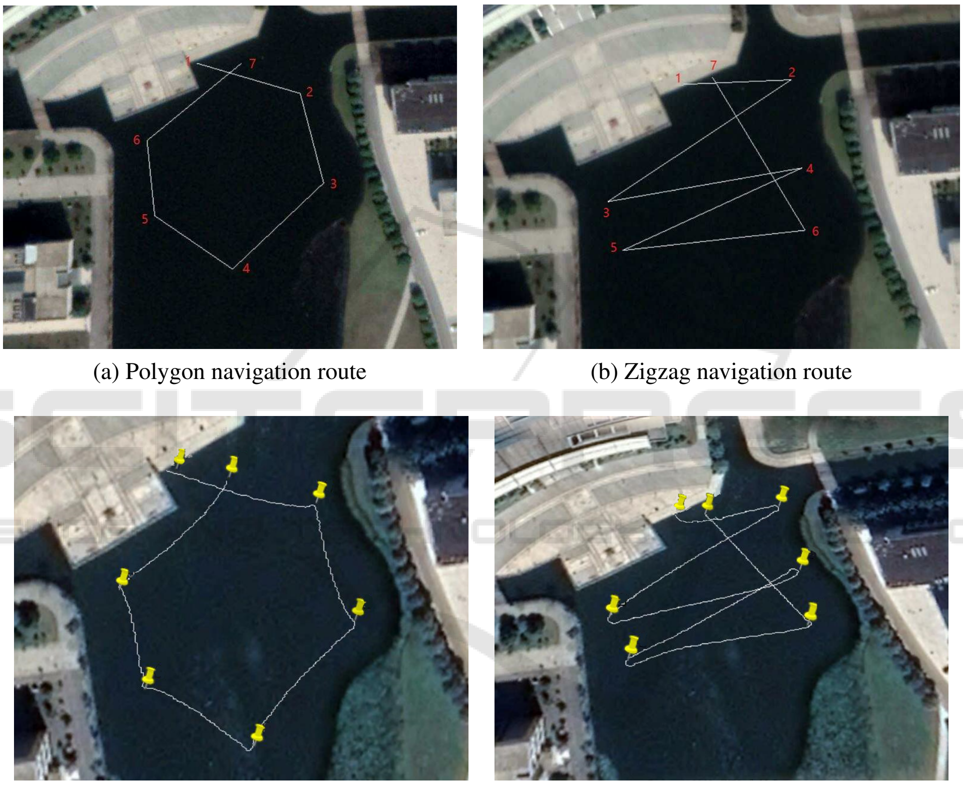

(a) Polygon navigation route

(b) Zigzag navigation route

(c) Actual track for polygon navigation route

(d) Actual track for zigzag navigation route

Figure 10: Autonomous navigation without obstacles.

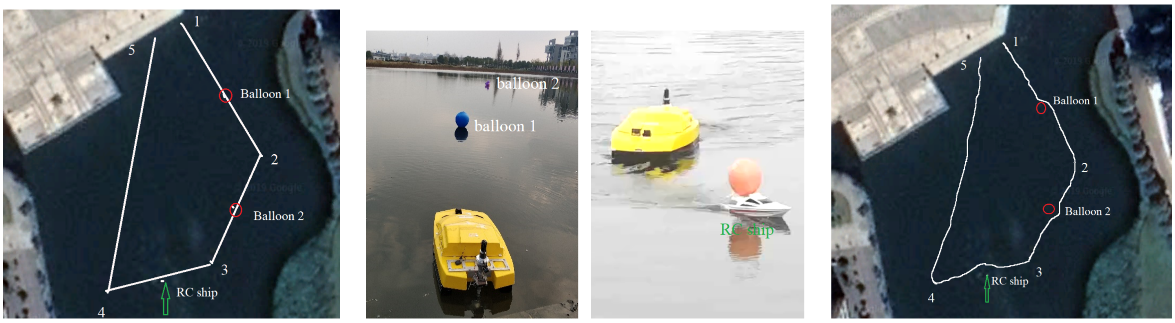

(a) Navigation route with obstacles

(b) USV, balloons and RC ship

(c) Actual track

Figure 11: Autonomous navigation with obstacles.

6 CONCLUSIONS

We proposed an improved APFM for USVs. A reversed obstacle avoidance algorithm was developed to improve the steering ability of the USV in tight spaces. Integrated with multi-position path planning approach and PID control, we simulated and tested the improved APFM in MATLAB to validate the correctness and performance of our algorithm. Finally, we applied our algorithm to a real USV and tested in a real lake. Experimental results show that the USV can autonomously navigate based on the predefined navigation route and avoid static and dynamic obstacles.

ACKNOWLEDGEMENTS

This work was partly supported by the AI University Research Centre (AI-URC) through XJTLU Key Programme Special Fund (KSF-P-02), Natural Science Foundation of Suzhou City (SYG201837), Natural Science Foundation of Nantong City(JC2018075)and Nantong University-Nantong Joint Research Center for Intelligent Information Technology (KFKT2017A06).

REFERENCES

Bertram, V. (2008). Unmanned surface vehicles-a survey. *Skibsteknisk Selskab, Copenhagen, Denmark*, 1:1–14.

Borenstein, J. and Koren, Y. (1990). Real-time obstacle avoidance for fast mobile robots in cluttered environments. In *Proceedings., IEEE International Conference on Robotics and Automation*, pages 572–577. IEEE.

Enderle, B., Yanagihara, T., Suemori, M., Imai, H., and Sato, A. (2004). Recent developments in a total unmanned integration system. In *Proc. AUVSI Unmanned Systems Conference*, volume 9.

Khatib, O. (1986a). Real-time obstacle avoidance for manipulators and mobile robots. In *Autonomous robot vehicles*, pages 396–404. Springer.

Khatib, O. (1986b). Real-time obstacle avoidance for manipulators and mobile robots. In *Autonomous robot vehicles*, pages 396–404. Springer.

Li, Y. and He, K. (2006). A novel obstacle avoidance and navigation method for outdoor mobile robot based on laser radar. *Robot*, 28(3):275–278.

Li, Z., Bachmayer, R., and Vardy, A. (2017). Vector field path following control for unmanned surface vehicles. In *OCEANS 2017-Aberdeen*, pages 1–9. IEEE.

Liu, Y., Liu, W., Song, R., and Bucknall, R. (2017). Predictive navigation of unmanned surface vehicles in a dynamic maritime environment when using the fast marching method. *International Journal of Adaptive Control and Signal Processing*, 31(4):464–488.

Liu, Z., Zhang, Y., Yu, X., and Yuan, C. (2016). Unmanned surface vehicles: An overview of developments and challenges. *Annual Reviews in Control*, 41:71–93.

Maguer, A., Gourmelon, D., Adatte, M., and Dabe, F. (2005). Flash and/or flash-s dipping sonars on spartan unmanned surface vehicle (usv): A new asset for littoral waters. In *Turkish International Conference on Acoustics*.

Manley, J. E. (2008). Unmanned surface vehicles, 15 years of development. In *OCEANS 2008*, pages 1–4. Ieee.

Naeem, W., Xu, T., Sutton, R., and Tiano, A. (2008). The design of a navigation, guidance, and control system for an unmanned surface vehicle for environmental monitoring. *Proceedings of the Institution of Mechanical Engineers, Part M: Journal of Engineering for the Maritime Environment*, 222(2):67–79.

Peng, Y., Han, J.-d., and Huang, Q.-j. (2009). Adaptive ukf based tracking control for unmanned trimaran vehicles. *International Journal of Innovative Computing, Information and Control*, 5(10):3505–3516.

Polvara, R., Sharma, S., Wan, J., Manning, A., and Sutton, R. (2018a). Obstacle avoidance approaches for autonomous navigation of unmanned surface vehicles. *The Journal of Navigation*, 71(1):241–256.

Polvara, R., Sharma, S., Wan, J., Manning, A., and Sutton, R. (2018b). Obstacle avoidance approaches for autonomous navigation of unmanned surface vehicles. *The Journal of Navigation*, 71(1):241–256.

Wang, H., Wei, Z., Wang, S., Ow, C. S., Ho, K. T., and Feng, B. (2011). A vision-based obstacle detection system for unmanned surface vehicle. In *2011 IEEE 5th International Conference on Robotics, Automation and Mechatronics (RAM)*, pages 364–369. IEEE.

Zhang, R., Tang, P., Su, Y., Li, X., Yang, G., and Shi, C. (2014a). An adaptive obstacle avoidance algorithm for unmanned surface vehicle in complicated marine environments. *IEEE/CAA Journal of Automatica Sinica*, 1(4):385–396.

Zhang, R., Tang, P., Su, Y., Li, X., Yang, G., and Shi, C. (2014b). An adaptive obstacle avoidance algorithm for unmanned surface vehicle in complicated marine environments. *IEEE/CAA Journal of Automatica Sinica*, 1(4):385–396.

Zhou, X., Ling, L., Ma, J., Tian, H., Yan, Q., Bai, G., Liu, S., and Dong, L. (2015). The design and application of an unmanned surface vehicle powered by solar and wind energy. In *Power Electronics Systems and Applications (PESA), 2015 6th International Conference on*, pages 1–10. IEEE.